Generalized parton distributions and description of electromagnetic and graviton form factors of nucleon

O. V. Selyugin and O. V. Teryaev

Bogoliubov Laboratory of Theoretical Physics, Joint Institute for Nuclear Research, 141980 Dubna, Moscow region, Russia

(Received 16 October 2008; published 3 February 2009)

A new parametrization of the generalized parton distributions t dependence is proposed. It allows one to reproduce sufficiently well electromagnetic form factors of the proton and neutron at small and large momentum transfer. The description of the data obtained by the Rosenbluth method and the polarization method are compared. The results obtained by the latter method are shown to be compatible with correspondent neutron data. The impact parameter dependence of the neutron charge density is examined. The quark contributions to gravitational form factors of the nucleons are obtained.

DOI: 10.1103/PhysRevD.79.033003 PACS numbers: 13.40.Gp, 12.38.Lg, 14.20.Dh

I. INTRODUCTION

The description of the hadron structure is related with our understanding of the nonperturbative properties of QCD. The essential part of the information about this structure is contained in the matrix elements of conserved quark operators.

The electromagnetic current of a nucleon is

$$J_\mu(P', s'; P, s) = \bar{u}(P', s')\Lambda_\mu(q, P)u(P, s) = \bar{u}(P', s')(\gamma_\mu F_1(q^2)) + \frac{1}{2M} i\sigma_{\mu\nu}q_\nu F_2(q^2))u(P, s), \quad (1)$$

where P, s, (P', s') are the four-momentum and polarization of the incoming (outgoing) nucleon and $q = P' - P$ is the momentum transfer. The quantity $\Lambda_\mu(q, P)$ is the nucleon-photon vertex.

Similar expressions for the decomposition of matrix elements of energy-momentum tensors describe the partition of angular momenta [1] and coupling of quarks and gluons to classical gravity [2]. The latter connection manifests also a relation to the equivalence principle for spin-gravity interactions [3–6] and its possible validity separately for quarks and gluons [7,8].

Two important combinations of the Dirac and Pauli form factors are the so-called Sachs form factors [9]:

$$G_E^p(t) = F_1^p(t) + \frac{t}{4M^2}F_2^p(t); \quad (2)$$

$$G_M^p(t) = F_1^p(t) + F_2^p(t); \quad (3)$$

with $t = -q^2 < 0$. Their three-dimensional Fourier transform provides the electric-charge-density and the magnetic-current-density distribution [10]. Normalization requires $G_E^p(0) = 1$, $G_E^n(0) = 0$ corresponding to proton and neutron electric charges; $G_M(0) = (G_E(0) + k) = \mu$ defines the proton and neutron magnetic moments. Here $\mu_p = (1 + 1.79)\frac{e}{2M}$ is the proton magnetic moment and $k = F_2(0)$ is the anomalous magnetic moment: $k_p = 1.79$

Early experiments at modest t, based on the Rosenbluth separation method, suggested the scaling behavior of both proton form factors and the neutron magnetic form factor approximately described by a dipole form,

$$G_E^p \approx \frac{G_M^p}{\mu_p} \approx \frac{G_M^n}{\mu_n} \approx G_D = \frac{\Lambda^4}{(\Lambda^2 - t)^2}, \quad (4)$$

which leads to

$$F_1^D(t) = \frac{4M_p^2 - t\mu_p}{4M_p^2 - t}G_D; \quad (5)$$

$$F_2^D(t) = \frac{4k_pM_p^2}{(4M_p^2 - t]}G_D; \quad (6)$$

with $\Lambda^2 = 0.71$ GeV^2. These experiments were based on the Rosenbluth formula [11],

$$\frac{d\sigma}{d\Omega} = \frac{\sigma_{\text{Mott}}}{\epsilon(1 + \tau)}[\tau G_M^2(t) + \epsilon G_E^2(t)], \quad (7)$$

where $\tau = Q^2/4M_p^2$ and $\epsilon = [1 + 2(1 + \tau)\tan^2(\theta_e/2)]^{-1}$ is a measure of the virtual photon polarization.

Recently, better data have been obtained by using of the polarization method [12,13]. Measuring both transverse and longitudinal components of the recoil proton polarization in the electron scattering plane, the data on the ratio

$$\frac{G_E^p}{G_M^p} = -\frac{P_t}{P_l}\frac{E + E'}{2M_p}\tan(\theta/2) \quad (8)$$

were obtained. These data manifested a strong deviation from the scaling law and, consequently, disagreement with data obtained by the Rosenbluth technique. The results consist in an almost linear decrease of G_E^p/G_M^p. There were attempts to solve the problem by inclusion of additional radiative correction terms related to two-photon exchange approximations, for example [14]. In recent works [15,16] the box amplitude is calculated when the intermediate state is a proton or the Δ resonance. The results of the numerical estimation show that the present

calculation of radiative corrections can bring into better agreement the conflicting experimental results on proton electromagnetic form factors. Note, however, that the precise data of a Rosenbluth measurement of the proton form factors at $Q^2 4.10\ \mathrm{GeV}^2$ [17] lie so high that they require very large corrections to move them down to meet the polarization data.

The form factors are related to the first moments of the generalized parton distributions (GPDs) [1,18–20]. Generally, GPDs depend on the momentum transfer t, the average momentum fraction $x = 0.5(x_i + x_f)$ of the active quark, and the skewness parameter $2\xi = x_f - x_i$ measures the longitudinal momentum transfer. One can choose the special case $\xi = 0$ of the nonforward parton densities [21] $\mathcal{F}^q_\xi(x; t)$ for which the emitted and reabsorbed partons carry the same momentum fractions:

$$\mathcal{H}^q(x, t) = H^q(x, 0, t) - H^{\bar{q}}(-x, 0, t), \tag{9}$$

$$\mathcal{E}^q(x, t) = E^q(x, 0, t) - E^{\bar{q}}(-x, 0, t). \tag{10}$$

The form factors can be represented as moments

$$F_1^q(t) = \int_0^1 dx \mathcal{H}^q(x, t), \tag{11}$$

$$F_2^q(t) = \int_0^1 dx \mathcal{E}^q(x, t), \tag{12}$$

following from the sum rules [1,19].

Nonforward parton densities also provide information about the distribution of the parton in impact parameter space [22] which is connected with t dependence of GPDs. Now we cannot obtain this dependence from the first principles, but it must be obtained from the phenomenological description with GPDs of the nucleon electromagnetic form factors.

Choosing a frame where the momentum transfer r is purely transverse $r = r_\perp$, the two-body contribution to the form factor can be written as [23]

$$F^{(2)}(t) = \int_0^1 dz \int_0^1 \Psi^*(x, k_\perp + \bar{x} r_\perp)\Psi(x, k_\perp)\frac{d^2 k_\perp}{16\pi^3}. \tag{13}$$

As it was shown in [21,24], assuming the Gaussian ansatz

$$\Psi(x; k_\perp) \sim \exp\left[-\frac{k_\perp^2}{2x(1-x)\lambda^2}\right], \tag{14}$$

one can obtain

$$F^{(2)}(q^2) = \int_0^1 dx q^{(2)}(x) e^{(1-x)q^2/4x\lambda^2}, \tag{15}$$

where $q^{(2)}(x)$ has the meaning of the two-body part of the quark density $q(x)$. The scale λ^2 characterizes the average transverse momentum of the valence quarks in the nucleon and $q^2 = -t$ is momentum transfer. This Gaussian ansatz was used in [21] for describing the form factors of proton. However, this ansatz leads to a faster decrease in F_1 at large momentum transfer. So there arises an important question about t dependence of GPDs.

In [25], it was proposed to use the factorized Regge-like picture

$$\mathcal{H}^q(x, t) \sim \frac{1}{x^{\alpha' t}} q(x), \tag{16}$$

which, however [24], does not satisfy some conditions in the light-cone representation.

In [26,27], two parts of $\Psi(x, k_\perp)$ were introduced which are responsible for the interaction at small momentum transfer $\Psi(x, k_\perp)^{\mathrm{soft}}$ and for the interactions at large momentum transfer $\Psi(x, k_\perp)^{\mathrm{hard}}$. These functions can reproduce the t dependence of, for example, F_1 but at the cost of the complicated mechanism and growth of F_1 at higher value of t.

In [24], the Regge-like picture was used again but now without factorization

$$\mathcal{H}^q(x, t) \sim \frac{1}{x^{\alpha'(1-x)t}} q(x). \tag{17}$$

This ansatz reproduces the basic properties of F_1 and provides a good description of the ratio of F_1 to F_2 and, consequently, of the ratio of G_E to G_M. A similar approach was examined in [28] with GPDs form $\sim(x/g_0)^{-\alpha(t)(1-x)}$, where $\alpha(t)$ is the nonlinear part of the Regge trajectory.

Note that in [29,30] it was shown that at large $x \to 1$ and momentum transfer the behavior of GPDs requires a larger power of $(1 - x)$ in the t-dependent exponent:

$$\mathcal{H}^q(x, t) \sim \exp[a(1-x)^n t] q(x), \tag{18}$$

with $n \geq 2$. It was noted that $n = 2$ naturally leads to the Drell-Yan-West duality between parton distributions at large x and the form factors.

In other works (see e.g. [31–33]) the description of the t dependence of the GPDs was developed in a more complicated picture using the polynomial forms:

$$\mathcal{H}^q(x, t) \sim q(x) \exp[f(x)t], \tag{19}$$

with

$$f(x) = \alpha'(1-x)^2 \ln\left(\frac{1}{x}\right) + B_q(1-x)^2 + A_q x(1-x) \tag{20}$$

or

$$f(x) = \alpha'(1-x)^3 \ln\left(\frac{1}{x}\right) + B_q(1-x)^3 + A_q x(1-x)^2. \tag{21}$$

These parametrizations provide the good description of the data extracted from [34]. The curve from Fig. 6 in [31]

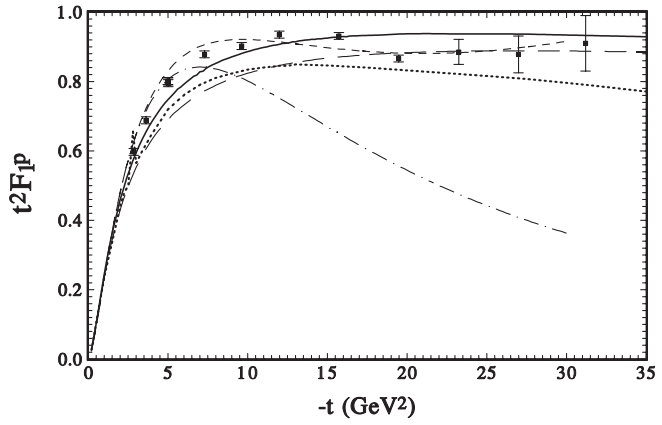

FIG. 1. Proton Dirac form factor multiplied by t^2 (hard line, the present work; dot-dashed line, [21]; long-dashed line, [24]; dashed line, [27]; dotted line, [31]; the data for F_1^p are from [45].

is reproduced in Fig. 1. Note, that the parametrization of (forward) parton distribution $q(x)$ there also differs from the other curves at Fig. 1.

II. NEW MOMENTUM TRANSFER DEPENDENCE OF GPDS

Let us modify the original Gaussian ansatz in order to incorporate the observations of [21,30] and choose the t dependence of GPDs in the form

$$\mathcal{H}^q(x,t) = q(x)\exp\left[a_+\frac{(1-x)^2}{x^m}t\right]. \tag{22}$$

The value of the parameter $m = 0.4$ is fixed by the low t experimental data while the free parameters $a_\pm$ (a_+—for $\mathcal{H}$ and a_-—for $\mathcal{E}$) were chosen to reproduce the experimental data in the whole t region. Indeed, large t behavior corresponds to $x \sim 1$ in (10) and (11), where the dependence on m is weak.

The function $q(x)$ was chosen at the same scale $\mu^2 = 1$ as in [24], which is based on the MRST2002 global fit [35]. In all our calculations we restrict ourselves, as in other quoted works, to the contributions of u and d quarks.

Hence, we have

$$u(x) = 0.262x^{-0.69}(1-x)^{3.50}(1 + 3.83x^{0.5} + 37.65x), \tag{23}$$

$$d(x) = 0.061x^{-0.65}(1-x)^{4.03}(1 + 49.05x^{0.5} + 8.65x). \tag{24}$$

Following the standard representation, see for example [24], we have for the Pauli form factor F_2

$$\mathcal{E}^q(x,t) = \mathcal{E}^q(x)\exp\left[a_-\frac{(1-x)^2}{x^{0.4}}t\right], \tag{25}$$

with

$$\mathcal{E}^u(x) = \frac{k_u}{N_u}(1-x)^{\kappa_1}u(x), \tag{26}$$

$$\mathcal{E}^d(x) = \frac{k_d}{N_d}(1-x)^{\kappa_2}d(x), \tag{27}$$

where $\kappa_1 = 1.53$ and $\kappa_2 = 0.31$ [24].

According to the normalization of the Sachs form factors, we have

$$k_u = 1.673, \qquad k_d = -2.033,$$
$$N_u = 1.53, \qquad N_d = 0.946.$$

The parameters $a_+ = 1.1$ and a_- were chosen to obtain two possible forms of the ratio of the Pauli and Dirac form factors. Below we consider variant (I) with $a_- = 1.1$ and variant (II) with $a_- = 1.4$ which correspond to the description of the experimental data obtained by the polarization method and the Rosenbluth method, respectively.

III. PROTON FORM FACTORS

The proton Dirac form factor, multiplied by t^2, is shown in Fig. 1 in comparison with other works and the experimental data. It can be seen that the complicated mechanism proposed in [26] leads to an increase in these values at higher t. One can see that our model reproduces sufficiently well the behavior of the experimental data at both high t and low t.

The ratio of the Pauli to the Dirac proton form factors multiplied by t is shown in Fig. 2. As mentioned above, there are two different sets of experimental data. Here we are not going to discuss these two methods and different corrections to them. We just observe that our model describes the results of both methods by changing the slope of $\mathcal{E}$ only and present two respective variants of this slope $a_\pm$.

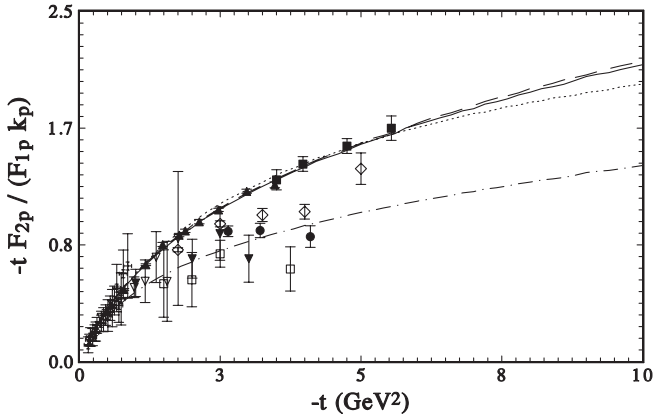

FIG. 2. Ratio of the Pauli to Dirac proton form factor multiplied by t [hard and dot-dashed lines correspond to variant (I) and (II)] of the present work, dotted line, [46]; long-dashed line, [24]); the data are from [47–50].

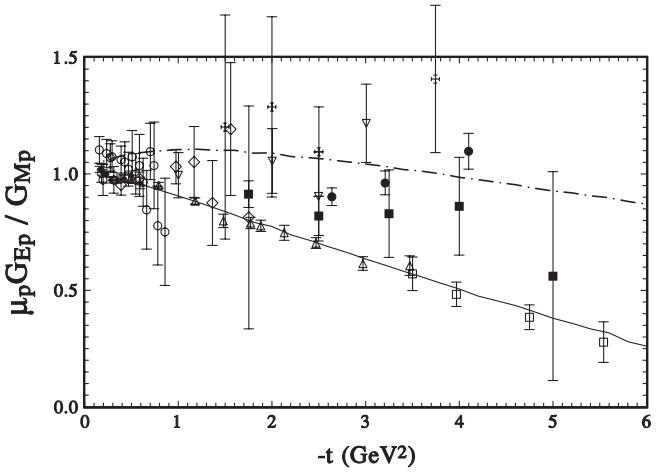

FIG. 3. $\mu_p G_E^p/G_M^p$ [hard and dot-dashed lines correspond to variant (I) and (II)]; the experimental data from [17,48–54].

This is supported also by Fig. 3 where $\mu_p G_E^p/G_M^p$ are shown in comparison with the experimental data.

IV. NEUTRON FORM FACTORS

Let us now calculate the neutron form factors using the model developed for the proton. The isotopic invariance can be used to relate the proton and neutron GPDs. Hence, we do not change any parameter and keep the same t dependence of GPDs as in the case of proton

$$\mathcal{H}^n(x,t) = q_+(x)_n \exp\left[2a_+ \frac{(1-x)^2}{x^{0.4}} t\right], \qquad (28)$$

where

$$q_+(x)_n = \tfrac{2}{3}d - \tfrac{1}{3}u. \qquad (29)$$

For the Pauli form factors of the neutron we correspondingly have

$$\mathcal{E}^n(x,t) = q_-(x)_n \exp\left[2a_- \frac{(1-x)^2}{x^{0.4}} t\right], \qquad (30)$$

with

$$q_-(x)_n = -\frac{1}{3}\frac{k_u}{N_u}(1-x)^{\kappa_1} u(x) + \frac{2}{3}\frac{k_d}{N_d}(1-x)^{\kappa_2} d(x). \qquad (31)$$

We take the two values of slope a_- as in the case of the proton form factors, corresponding to variant (I) and variant (II) below.

First, let us calculate G_E^n. The results are shown in Fig. 4. Evidently, the first variant is in better agreement with the experimental data.

A more clear situation with our calculations of G_M^n is shown in Fig. 5. In this case, it is obvious that the first variant much better describes the experimental data, especially at low momentum transfer.

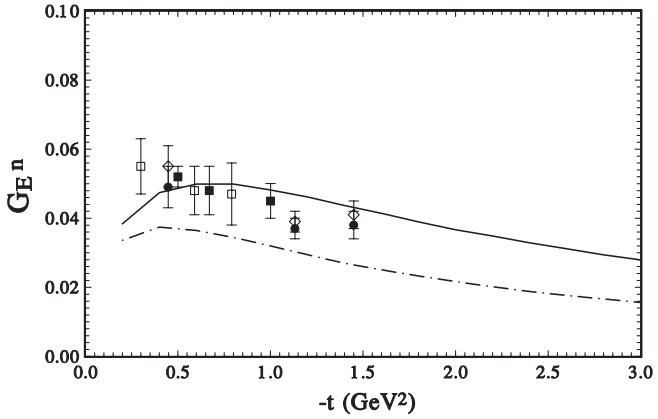

FIG. 4. G_E^n [hard and dot-dashed lines correspond to variant (I) and (II)]; the experimental data are from [55–57].

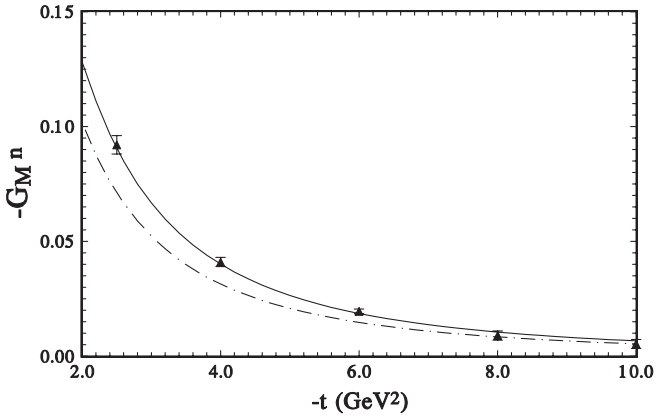

FIG. 5. G_M^n [hard and dot-dashed lines correspond to variant (I) and (II)]; the experimental data are from [58].

Finally, we present our calculations for the ratio of G_E^n/G_M^n for neutron in Fig. 6.

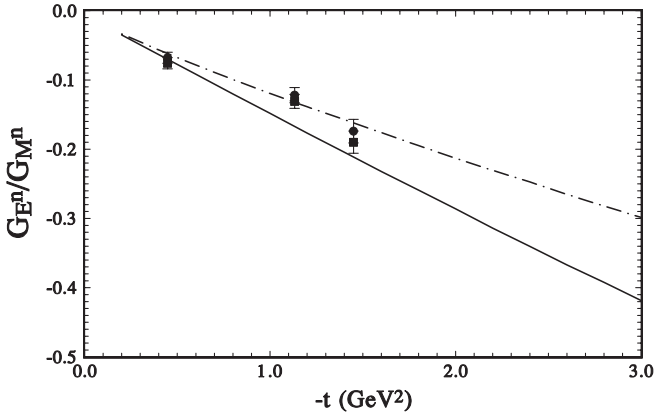

FIG. 6. G_E^n/G_M^n [hard and dot-dashed lines corresponds to variant (I) and (II)]; experimental data are from [55,56].

V. CHARGE DENSITIES OF NEUTRON

Let us now discuss the neutron structure in the impact parameter [36–38] representation. We are particularly motivated by a recent discussion of the definition of charge density of the neutron at small impact parameters corresponding to the ''center'' of the neutron [39,40]. In [40], the charge density of the neutron is related to $F_1^n(t)$ and calculated using phenomenological representation of the $G_E^n(t)$ and $G_M^n(t)$:

$$\rho(b) = \sum_q e_q \int dx q(x,b) \qquad = \int d^2q F_1(Q^2 = q^2) e^{i\vec{q}\,\vec{b}}$$
$$= \int_0^\infty \frac{qdq}{2\pi} J_0(qb) \frac{G_E(q^2) + \tau G_M(q^2)}{1+\tau}, \tag{32}$$

J_0 being a cylindrical Bessel function. It differs essentially from the definition of the neutron charge distribution in the Breit frame related $G_E^n(t)$:

$$\rho_{G_E}(b) = \int d^2q [F_1(q^2) + \tau F_2(q^2)] e^{i\vec{q}\,\vec{b}}$$
$$= \int_0^\infty \frac{qdq}{2\pi} J_0(qb) G_E(q^2). \tag{33}$$

Using our model of t dependence of GPDs, we may calculate both forms of neutron charge distribution in the impact parameter representation and, moreover, determine separate contributions of u and d quarks.

The charge distribution $\rho_n(b)$ corresponding to G_E^n is shown in Fig. 7. It practically coincides with the result [41]. The charge density of the neutron $\rho_n(b)$ corresponding to F_1 is shown in Fig. 8, while the respective separate contributions of u and d quarks are shown in Fig. 9. We can see that u quarks have the large negative charge density in the center of the neutron.

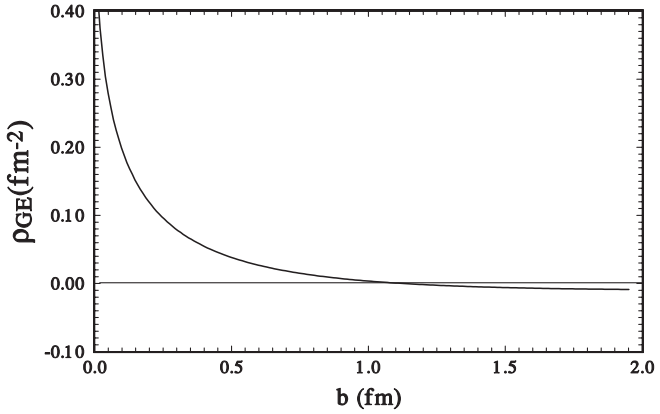

FIG. 7. Parton charge density of the neutron $\rho_n(b)$ corresponds to $G_E(b)$.

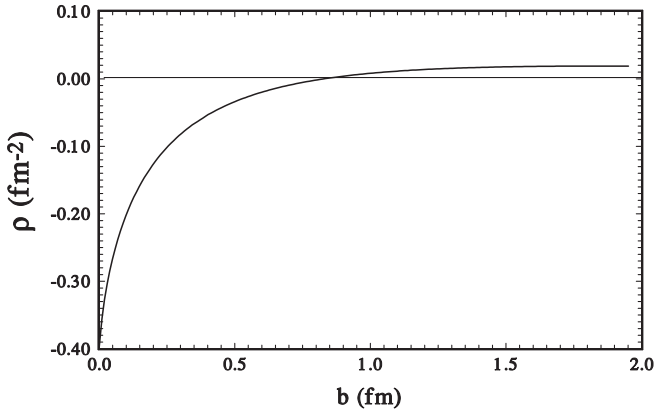

FIG. 8. Parton charge density of the neutron $\rho_n(b)$ corresponds to $F_1(b)$.

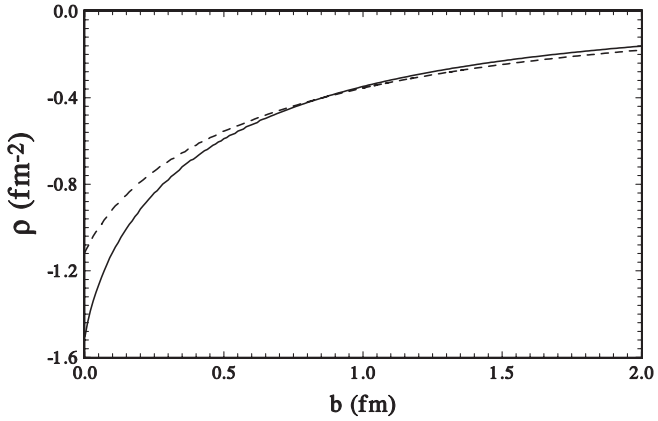

FIG. 9. u-quark (hard line) and $(-d)$-quark (dashed line) density of the neutron.

VI. TRANSVERSE CHARGE DENSITIES

Recently, the impact parameter distributions were generalized [42] to the case of spin-flip magnetic form factor so that in addition to expression (32) one has

$$\rho_T^N(\vec{b}) = \rho_0^N(\vec{b}) + \sin(\phi) \frac{1}{2\pi} \int_0^\infty dq \frac{q^2}{2M_N} J_1(qb) F_2(q^2), \tag{34}$$

here $\tan(\phi) = b_x/b_y$. This transverse charge density for the proton obtained in the framework of our model is shown in Fig. 10 while the angular-dependent contribution [second term in (34)] is shown in Fig. 11.

The angular-dependent part of the density is small and it is practically invisible in Fig. 10. However, removing the axially symmetric part of the density related to $\rho_0^N(\vec{b})$, one can see that the nonsymmetric part is reaching the value about ± 0.05 (see Fig. 11) at the distance of 0.3 fm from the center of the proton, comparable to the size of the valence quark.

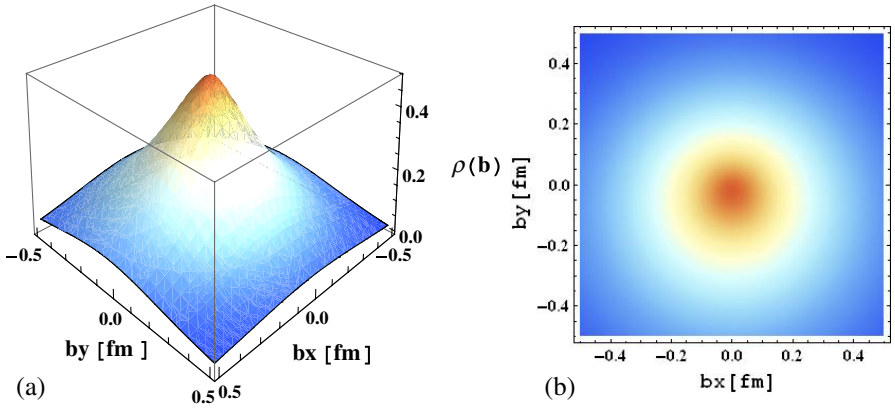

FIG. 10 (color online). Quark transverse charge density of the proton Eq. (34): (a) left panel, back side view; (b) right panel, view from above.

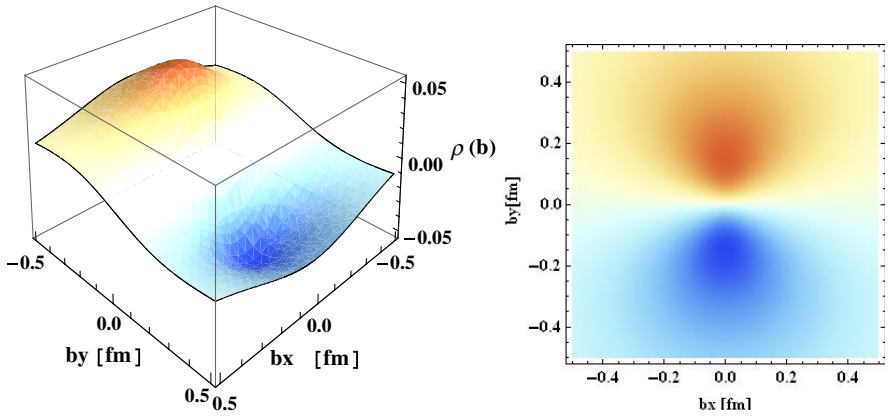

FIG. 11 (color online). Angular-dependent contribution to quark transverse charge density of the proton $\rho_T^p(\vec{b}) - \rho_0^p(\vec{b})$: (a) left panel, back side view; (b) right panel, view from above.

The transverse densities of the neutron is presented in Figs. 12 and 13. In this case the symmetric part of the transverse density $\rho_0^n(\vec{b})$ is small (compare with Fig. 8). while the nonsymmetric part is sufficiently large and concentrated around the center of the neutron.

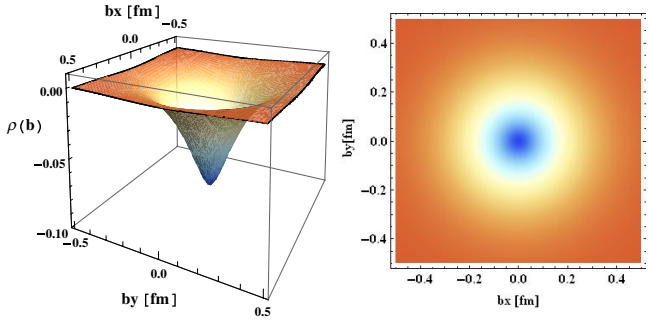

FIG. 12 (color online). Quark transverse charge densities of the neutron $\rho_0^n(\vec{b})$: (a) left panel, with the back side view point; (b) right panel, with the upper view point.

VII. GRAVITATIONAL FORM FACTORS

Taking the matrix elements of energy-momentum tensor $T_{\mu\nu}$ instead of the electromagnetic current J^μ, one can obtain the gravitational form factors of quarks which are related to the second, rather than the first moments of GPDs:

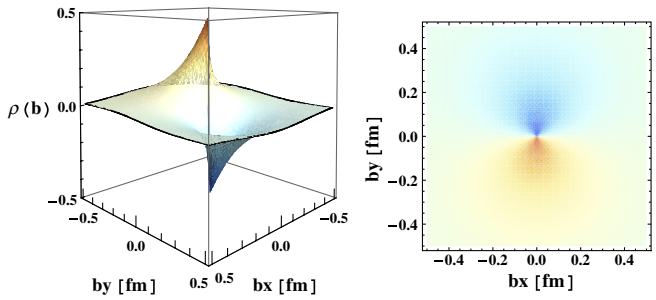

FIG. 13 (color online). Quark transverse charge densities of the neutron $\rho_T^N(\vec{b}) - \rho_0^N(\vec{b})$: (a) left panel, with the back side view point; (b) right panel, with the upper view point.

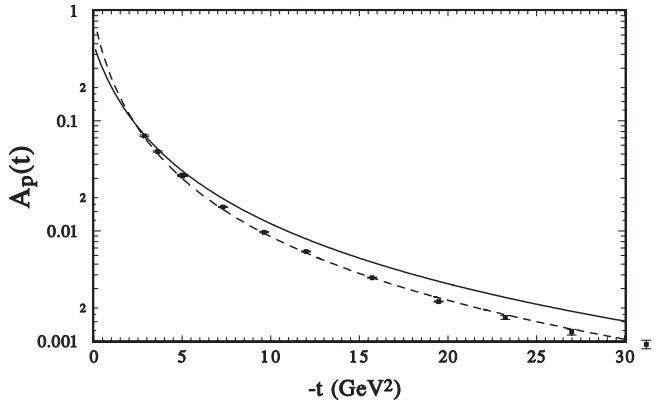

FIG. 14. Comparison of gravitational form factor A_{u+d} (hard line) and proton Dirac form factor (dashed line) multiplied by t^2, the data for F_1^p are from [45].

$$\int_{-1}^{1} dx x H_q(x, \Delta^2, \xi) = A_q(\Delta^2);$$
$$\int_{-1}^{1} dx x E_q(x, \Delta^2, \xi) = B_q(\Delta^2). \tag{35}$$

For $\xi = 0$ one has

$$\int_0^1 dx x \mathcal{H}_q(x, t) = A_q(t); \qquad \int_0^1 dx x \mathcal{E}_q(x, t) = B_q(t). \tag{36}$$

This representation combined with our model (we use here the first variant of parameters describing the experimental data obtained by the polarization method) allows one to calculate the gravitational form factors of valence quarks and their contribution (being just their sum) to gravitational form factors of the nucleon. Our result for $A_{u+d}(t)$ is shown in Fig. 14. Separate contributions of the u and d quark distribution are shown in Fig. 15. At $t = 0$ these contributions equal $A_u(t = 0) = 0.35$ and $A_d(t = 0) = 0.14$. The corresponding calculations for $B_q(t)$ are shown in Fig. 16. At $t = 0$ these contributions equal

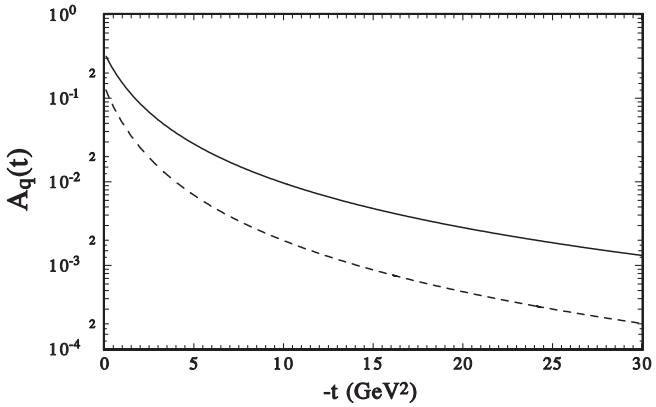

FIG. 15. Contributions of the u quark (hard line) and d quark (dashed line) to the gravitational form factor A_q.

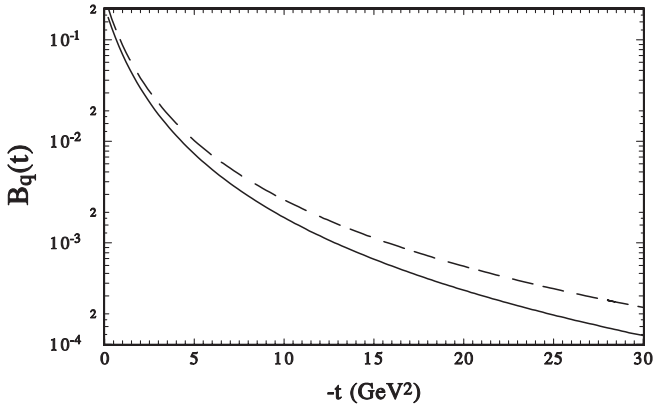

FIG. 16. Contributions of the u (hard line) and d (with reversed sign; dashed line) quarks to the gravitation form factor B_q.

$B_u(t = 0) = 0.22$ and $B_d(t = 0) = -0.27$. Hence, their sum shows the sort of compensation supporting the conjecture [7,8] about validity of the equivalence principle separately for quarks and gluons: $B_{u+d}(t = 0) = -0.05$.

Note that nonperturbative analysis within the framework of the lattice QCD indicates that the net quark contribution to the anomalous gravitomagnetic moment $B_{u+d}(0)$ is close to zero [43,44].

Let us compare the distribution of electric charge and matter (that is, gravitational charge) in the nucleon. For that purpose we generalize (34) in a straightforward way and introduce the gravitomagnetic transverse density

$$\rho_T^{\mathrm{Gr}}(\vec{b}) = \rho_0^{\mathrm{Gr}}(b) + \sin(\phi)\frac{1}{2\pi}\int_0^\infty dq \frac{q^2}{2M_N} J_1(qb) B(q^2), \tag{37}$$

with a matter density

$$\rho_0^{\mathrm{Gr}}(b) = \frac{1}{2\pi}\int_\infty^0 dq q J_0(qb) A(q^2). \tag{38}$$

In Fig. 17 we compare this matter density with the charge density (cf. Sec. V) for proton. The plots for the angular-dependent part of transverse density $\rho_T^{\mathrm{Gr}}(\vec{b}) - \rho_0^{\mathrm{Gr}}(b)$ are shown in Figs. 18 and 19. One can see that it is quite small

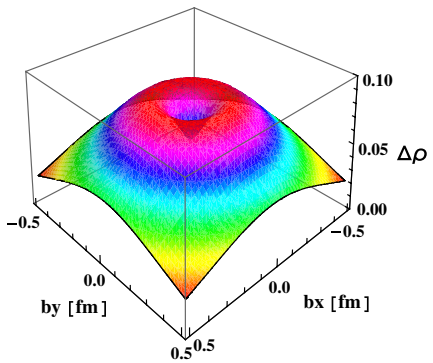

FIG. 17 (color online). Difference in the forms of charge density F_1^P and "matter" density (A).

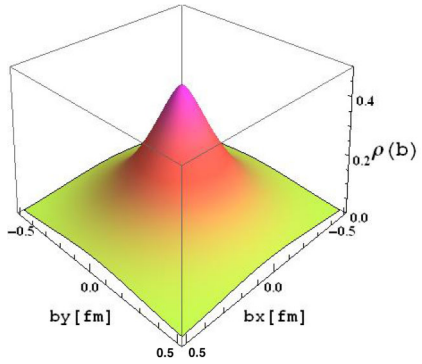

FIG. 18 (color online). Densities of gravitational form factor A.

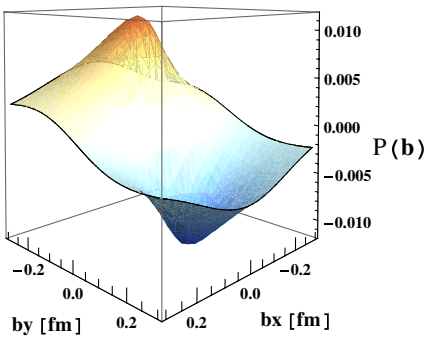

FIG. 19 (color online). Transverse density $\rho_T^{\mathrm{Gr}}(\vec{b}) - \rho_0^{\mathrm{Gr}}(b)$.

and its maximal values are concentrated almost at the same distances from the center of nucleon as the transverse charge density of the proton.

VIII. CONCLUSION

We introduced a simple new form of the GPDs t dependence based on the Gaussian ansatz corresponding to that of the wave function of the hadron. It satisfies the conditions of the nonfactorization, introduced by Radyushkin, and the Burkhardt condition on the power of $(1-x)^n$ in the exponential form of the t dependence. With this simple form we obtained a good description of the proton electromagnetic form factors. Using the isotopic invariance, we obtained also a good description of the neutron Sachs form factors without changing any parameters. We showed that both sets of the experimental data (obtained by the Rosenbluth and polarization methods) on the electromagnetic form factors can be described by changing only the slope of the t dependence of the spin-dependent GPD $\mathcal{E}(x, t)$. Comparison of these two variants with the neutron form factors gives preference to the one which describes data obtained by the polarization method.

Our calculations of charge distribution of the neutron in the impact parameter form of F_1 coincide with the calculation by Miller obtained from phenomenological forms of G_E^p and G_M^p. They confirm that respective charge density is negative at small impact parameters. On the basis of our results we calculated the contribution of u and d quarks to the gravitational form factor of the nucleons. The cancellation of these contributions at $t = 0$ shows that the gravitomagnetic form factor is close to zero for separate contributions of gluons and quarks, which supports the conjecture of [7,8].

ACKNOWLEDGMENTS

The authors would like to thank M. Anselmino and E. Predazzi for helpful discussion. The visit of O. S. to Torino was supported by the INFN-LTPh(JINR) agreement program. This work was supported in part by Grants No. RFBR 06-02-16215 and No. RF MSE RNP 2.2.2.2.6546.

[1] X. D. Ji, Phys. Rev. Lett. **78**, 610 (1997); Phys. Rev. D **55**, 7114 (1997).
[2] O. V. Teryaev, arXiv:hep-ph/9904376.
[3] I. Yu. Kobzarev and L. B. Okun, Zh. Eksp. Teor. Fiz. **43**, 1904 (1962); [Sov. Phys. JETP **16**, 1343 (1963)].
[4] S. J. Brodsky, Dae Sung Hwang, Bo-Qiang Ma, and Ivan Schmidt, Nucl. Phys. **B578**, 326 (2000).
[5] A. J. Silenko and O. V. Teryaev, Phys. Rev. D **71**, 064016 (R) (2005).
[6] A. J. Silenko and O. V. Teryaev, Phys. Rev. D **76**, 061101 (R) (2007).
[7] O. V. Teryaev, Czech. J. Phys. **53**, 47 (2003), Suppl. B.
[8] O. V. Teryaev, AIP Conf. Proc. **915**, 260 (2007).
[9] F. J. Ernst, R. G. Sachs, and K. C. Wali, Phys. Rev. **119**, 1105 (1960).
[10] R. G. Sachs, Phys. Rev. **126**, 2256 (1962).
[11] M. N. Rosenbluth, Phys. Rev. **79**, 615 (1950).
[12] A. I. Akhiezer and M. P. Rekalo, Sov. J. Pat. Nucl. **4**, 277 (1974); Fiz. Elem. Chast. Atom. Yadra (PEPAN) **4**, 662 (1973).
[13] R. G. Arnold, C. E. Carlson, and F. Gross, Phys. Rev. C **23**, 363 (1981).
[14] P. A. M. Guichon and M. Vanderhaeghen, Phys. Rev. Lett. **91**, 142303 (2003); P. G. Blunden, W. Melnitchouk, and A. Tjon, Phys. Rev. Lett. **91**, 142304 (2003); Y. C. Chen *et al.*, Phys. Rev. Lett. **93**, 122301 (2004); M. P. Recalo and E. Tomasi-Gustafssn, Eur. Phys. J. A **22**, 331 (2004); S. Dubnichka, E. Kuraev, M. Secansky, and A. Vinnikov, arXiv:hep-ph/0507242.
[15] Yu. M. Bystritsky, E. A. Kuraev, and E. Tomasi-Gustafsson, arXiv:hep-ph/0603132.
[16] E. A. Kuraev, V. V. Bytev, Yu. M. Bystritskiy, and E.

Tomasi-Gustafsson, Phys. Rev. D **74**, 013003 (2006).
[17] I. A. Qattan *et al.*, Phys. Rev. Lett. **94**, 142301 (2005).
[18] D. Muller, D. Robaschik, B. Geyer, F. M. Dittes, and J. Horejsi, Fortschr. Phys. **42**, 101 (1994).
[19] A. V. Radyushkin, Phys. Rev. D **56**, 5524 (1997).
[20] J. Collins, L. Frankfurt, and M. Strikman, Phys. Rev. D **56**, 2982 (1997).
[21] A. V. Radyushkin, Phys. Rev. D **58**, 114008 (1998).
[22] M. Burkardt, Phys. Rev. D **62**, 071503(R) (2000).
[23] S. J. Brodsky, T. Huang, and G. P. Lepage, in *Proceedings of the Banff Summer Institute, Bunff, Alberta, 1981*, edited by A. Z. Capri and A. N. Kamal (Plenum, New York, 1983), p. 143.
[24] M. Guidal, M. V. Polyakov, A. V. Radyushkin, and M. Vanderhaeghen, Phys. Rev. D **72**, 054013 (2005).
[25] K. Goeke, M. V. Polyakov, and M. Vanderhaeghen, Prog. Part. Nucl. Phys. **47**, 401 (2001).
[26] P. Stoler, Phys. Rev. D **65**, 053013 (2002).
[27] P. Stoler, Phys. Rev. Lett. **91**, 172303 (2003).
[28] L. Jenkovszky, Phys. Rev. D **74**, 114026 (2006).
[29] F. Yuan, Phys. Rev. D **69**, 051501(R) (2004).
[30] M. Burkardt, Phys. Lett. B **595**, 245 (2004).
[31] M. Diehl, Th Feldmann, R. Jakob, and P. Kroll, Eur. Phys. J. C **39**, 1 (2005).
[32] S. V. Goloskokov and P. Kroll, Eur. Phys. J. C **42**, 281 (2005).
[33] P. Kroll, AIP Conf. Proc. **904**, 76 (2007).
[34] E. J. Brash, A. Kozlov, S. Li, and G. M. Huber, Phys. Rev. C **65**, 051001 (2002).
[35] A. D. Martin *et al.*, Phys. Lett. B **531**, 216 (2002).
[36] M. Burkhardt, arXiv:0509316.
[37] D. E. Soper, Phys. Rev. D **15**, 1141 (1977).
[38] H. Dahiya, A. Mukherjee, and S. Ray, Phys. Rev. D **76**, 034010 (2007).
[39] M. Burkardt, arXiv:0709.2966v2.
[40] G. A. Miller, Phys. Rev. Lett. **99**, 112001 (2007); arXiv:0705.2409v2; arXiv:0802.2563v2.
[41] J. J. Kelly, Phys. Rev. C **66**, 065203 (2002).
[42] C. E. Carlson and M. Vanderhaeghen, Phys. Rev. Lett. **100**, 032004 (2008).
[43] M. Goeckeler *et al.*, Nucl. Phys. B, Proc. Suppl. **128**, 203 (2004).
[44] Ph. Hagler *et al.*, Eur. Phys. J. A **24**, 29 (2005).
[45] A. F. Sill *et al.*, Phys. Rev. D **48**, 29 (1993).
[46] S. J. Brodsky, arXiv:hep-ph/0208158.
[47] M. K. Jones *et al.*, Phys. Rev. Lett. **84**, 1398 (2000).
[48] O. Gayou *et al.*, Phys. Rev. C **64**, 038202 (2001).
[49] O. Gayou *et al.*, Phys. Rev. Lett. **88**, 092301 (2002).
[50] V. Punjabil *et al.*, Phys. Rev. C **71**, 055202 (2005).
[51] J. Arrington, Phys. Rev. C **71**, 015202 (2005).
[52] B. Hu *et al.*, Phys. Rev. C **73**, 064004 (2006).
[53] C. B. Grawford *et al.*, Phys. Rev. Lett. **98**, 052301 (2007).
[54] I. A. Qattan, Ph.D. thesis, Northwestern University, 2005 [arXiv:nucl-ex/0610006].
[55] B. Plaster *et al.*, Phys. Rev. C **73**, 025205 (2006).
[56] R. Madey *et al.*, Phys. Rev. Lett. **91**, 122002 (2003).
[57] I. G. Warren *et al.*, Phys. Rev. Lett. **92**, 042301 (2004).
[58] S. Rock *et al.*, Phys. Rev. Lett. **49**, 1139 (1982).